Neuropharmacology 132 (2018) 58–70

Contents lists available at ScienceDirect

Neuropharmacology

journal homepage: www.elsevier.com/locate/neuropharm

Invited review

Relevance of tissue specific subunit expression in channelopathies

Hartwig Seitter, Alexandra Koschak*

University of Innsbruck, Institute of Pharmacy, Pharmacology and Toxicology, Center for Chemistry and Biomedicine, Innrain 80-82/III, 6020 Innsbruck, Austria

ARTICLE INFO

Article history:
Received 1 March 2017
Received in revised form
22 June 2017
Accepted 28 June 2017
Available online 29 June 2017

Keywords:
Tissue expression
Calcium channel
Channelopathy
Retina
Congenitals stationary night blindness

ABSTRACT

Channelopathies are a diverse group of human disorders that are caused by mutations in genes coding for ion channels or channel-regulating proteins. Several dozen channelopathies have been identified that involve both non-excitable cells as well as electrically active tissues like brain, skeletal and smooth muscle or the heart. In this review, we start out from the general question which ion channel genes are expressed tissue-selectively. We mined the human gene expression database Human Protein Atlas (HPA) for tissue-enriched ion channel genes and found 85 genes belonging to the ion channel families. Most of these genes were enriched in brain, testis and muscle and a complete list of the enriched ion channel genes is provided. We further focused on the tissue distribution of voltage-gated calcium channel (VGCC) genes including different brain areas and the retina based on the human gene expression from the FANTOM5 dataset. The expression data is complemented by an overview of the tissue-dependent aspects of L-type calcium channel (LTCC) function, dysfunction and pharmacology, as well as of their splice variants. Finally, we focus on the pathology of tissue-restricted LTCC channelopathies and their treatment options.

This article is part of the Special Issue entitled 'Channelopathies.'

Contents

1. Introduction

The physiology and functionality of cell types and tissues is based on the underlying gene expression diversity within the different body parts of a living being. The question arises which of these genes are ubiquitously expressed and which genes and combinations endow organs with their unique tissue identity. In channelopathies, i.e. human pathologies caused by dysfunction of ion channels, the tissue-dependence can profoundly affect disease manifestation and treatment options.

Voltage-gated Ca^{2+} channels (VGCCs) are interesting case examples of ion channels that have very selective or very widespread tissue distribution. VGCCs generate Ca^{2+} signals for many important physiological functions such as neurotransmission, muscle contraction, hormone secretion as well as regulation of gene expression (Catterall, 2011). Like other ion channels they form part of signaling complexes together with molecules, such as receptors, kinases, phosphatases and calmodulin (Catterall, 2011). Most VGCCs exist in a hetero-oligomeric complex of several subunits

* Corresponding author.
E-mail address: alexandra.koschak@uibk.ac.at (A. Koschak).

http://dx.doi.org/10.1016/j.neuropharm.2017.06.029
0028-3908/

with the α1-subunit forming the Ca^{2+}-selective channel pore. Their biophysical and pharmacological properties are determined by their α1-subunit. Based on structural and pharmacological similarities of their α1-subunits, VGCCs can be grouped into two major families: LTCCs (Ca_v1 family; Cav1.1-Cav1.4) and non-LTCCs (Ca_v2, Cav2.1-Cav2.3; Ca_v3 families, Cav3.1-Cav3.3). The ten different α1-subunit isoforms associate with different β-subunits (β1-4) and α2δ subunits (α2δ1-4) and in some cases also γ-subunits. For a detailed overview we refer to a recent review by Zamponi and colleagues (Zamponi et al., 2015).

LTCC channelopathies are particularly interesting because some show obvious signs of tissue-selective phenotypes, whereas others are caused by less focally expressed channel genes that nevertheless primarily affect certain tissues. As for example skeletal muscle diseases like malignant hyperthermia or hypokalemic periodic paralysis (Jurkat-Rott et al., 2002) are caused by mutations in the very tissue-selectively expressed *CACNA1S* gene that encodes for Cav1.1 LTCCs. Also the *CACNA1F* gene that translates into Cav1.4 LTCCs exhibits very selective expression in the retina and therefore shows a tissue-specific disease manifestation (Zeitz et al., 2015). In contrast the two other LTCC members, Cav1.2 and Cav1.3 do not show a similar restriction of expression localization. Of note, some of their associated channelopathies (e.g. Timothy syndrome in Cav1.2) also highlight aspects of splice variant expression differences and the importance of the cellular environment for a phenotypic exhibition.

As 'channel diggers' we would highly benefit from a better overview of the tissue-selectivity of gene expression and/or even cell specific expression to unearth their functional mysteries.

2. Tissue specificity in voltage-gated ion channel genes according to large-scale screenings

Details on ion channel expression in single cell types are slowly accumulating. However it is also worthwhile to look at the overall ion channel repertoires on the tissue level from human transcriptome and proteome screenings. Recently large-scale screenings of human gene expression in tissues have been undertaken by several consortiums that allow for a broader view on gene expression localization in the human body (for an overview (Uhlen et al., 2016)). Here we made use of two datasets, the Human Protein Atlas (www.proteinatlas.org; (Uhlen et al., 2015)) and FANTOM5 (fantom.gsc.riken.jp/5/; (Lizio et al., 2015)). Within the framework of the Human Protein Atlas (HPA), Illumina-sequencing of RNA (RNA-seq) was performed on 32 human tissues, capturing the mRNA levels of transcripts within each tissue. Although mRNA level to protein level ratios can vary between different gene products depending on e.g. translation rates and protein half-life (Eden et al., 2011), overall the data from RNA-seq is in good agreement with corresponding protein amounts (Wilhelm et al., 2014). The genes contained in the HPA are categorized according to their tissue-selective expression. Of the putative 19628 protein coding genes, 7367 genes were classified as expressed in all tissues, while 7835 genes showed elevated expression in subsets of tissues (3328 were mixed, 1098 not detected). The most selectively expressed subclass among the elevated genes are so-called tissue-enriched genes (defined by an expression value in the highest-expressing tissue that is at least five-fold of the second highest expression value; tissue specificity score TS $\geq$ 5).

From the HPA list of 2547 tissue-enriched genes we pulled out the 85 genes that belong to the ion channel families (according to the IUPHAR ion channel list, (Southan et al., 2016)) to obtain an overview of which ion channels are expressed most selectively (Table 1) and could thus give rise to a tissue-specific ion channel function in health and disease. The majority of tissue-enriched ion channel genes were found in a low number of tissues. As expected, the four tissues with the most ion channel genes comprised electrically active tissues like cerebral cortex, skeletal muscle and heart, but also testis contained a number of selectively expressed ion channel genes (Fig. 1). Yet, the fraction of channel genes was different for these tissues. While testis contained the largest number of tissue-enriched genes (Fig. 1A), only few of those genes code for ion channels (Fig. 1B). Cerebral cortex, skeletal muscle and heart included a much higher fraction of ion channels that was comparable within these three tissues. Cerebral cortex displayed the second highest number of tissue-enriched genes, therefore most of the ion channels were indeed found there. In Fig. 1C the ion channel genes selectively expressed in cerebral cortex, testis, skeletal muscle and heart are summarized and sorted according to their expression strengths within the given tissue. The numbers refer to Table 1 to facilitate retrieval of additional information.

The dataset can be looked at in detail from different angles: which genes are found in a given tissue or which tissues express a certain gene? For the former we concentrated on VGCC expression in three different tissue subsets: brain regions, muscle tissues and lymphoid tissues (Fig. 2). It is evident that there is only partial selectivity of expression of individual VGCC subunits, e.g. $Ca_V1.1$ and $Ca_V1.4$ LTCCs which show a very restricted expression in skeletal muscle and retinal tissue, respectively (Fig. 2A). Ca_V2 channels and γ subunits showed an overall CNS-focused expression pattern. The most striking differences in the FANTOM5 brain samples were seen with respect to $Ca_V2.1$ which was highly expressed in the cerebellum and $Ca_V2.3$ that was most prominent in caudate (Fig. 2B). In general, the human data compared well with the data from mouse brain samples; e. g. evidence from quantitative RT-PCR analyses in hippocampal and cerebellar tissue found similar relationships in $Ca_V2.1$, $Ca_V2.3$, β_4, $\alpha_2\delta$-1 and $\alpha_2\delta$-2 as in the FANTOM5 data, albeit e.g. $Ca_V1.3$ and β_2 showed a different ratio (Schlick et al., 2010).

In the muscle tissues a clear-cut segregation in the use of LTCCs and β-subunits was apparent. In skeletal muscle: $Ca_V1.1$ and β_1; in heart and smooth muscle: $Ca_V1.2$ and β_2; while all muscle tissues are alike in their expression of $\alpha_2\delta$-1 as the main $\alpha_2\delta$ subunit (Fig. 2C). Smooth muscle showed additionally high expression levels of $Ca_V3.2$ as has previously been demonstrated ((Harraz et al., 2015a; Harraz et al., 2015b), for review (Kuo et al., 2014). Other findings suggest that smooth muscle cells of the CNS vasculature also express Cav3.1 ((Fernandez et al., 2015), rat retina arterioles) and Cav3.3 (Harraz et al., 2015b), human cerebral arteries). The γ_1 subunit was only found in skeletal muscle but with a striking abundance (see inset in Fig. 2C for comparison of skeletal muscle VGCC subunit expression strengths). Overall this expression map recapitulated well what is known about muscle tissue Ca^{2+} channel repertoires (Catterall et al., 2005).

LTCCs have been reported repeatedly also in cells of the lymphoid lineage, mainly in different types of T-cells (for an overview, see (Davenport et al., 2015; Badou et al., 2013)). In the FANTOM5 lymphoid tissues the only LTCCs with prominent expression were $Ca_V1.2$ and $Ca_V1.3$ (Fig. 2D). Both have been described previously (Cabral et al., 2010; Robert et al., 2014). $Ca_V1.1$ (Matza et al., 2016) and $Ca_V1.4$ (Robert et al., 2014) (Omilusik et al., 2011; McRory et al., 2004) have also been reported in immune cells/tissues but were not detected in the FANTOM5 lymphoid tissues (with exception of a low amount of $Ca_V1.1$ in the tonsil tissue). It is unclear if this could be attributed to the activation state of the immune cells because $Ca_V1.4$ expression was reported in naive T-cells as well as upon activation (Omilusik et al., 2011), while a novel variant of $Ca_V1.1$ (lacking exon 29 like in embryonic skeletal muscle but with alternative N-terminal exons; Table 2 and see also below) was found in T-cells after T-cell receptor stimulation (Matza et al.,

Table 1
List of tissue-enriched channel genes in human tissues. We pulled out all ion channel genes (according to IUPHAR list of ion channel family members) from the dataset of tissue-enriched genes found in the Human Protein Atlas (HPA). Genes in the HPA tissue-enriched gene list have the highest selectivity of expression (expression in one tissue at least five-fold higher than all other tissues). In total, we found 85 channel genes, numbered from highest tissue specificity to lowest. Black squares indicate the tissue in which the gene is enriched. Abbreviations: a.k.a., also known as; TS, tissue specificity score; TPM, transcripts per million (expression strength in the indicated tissue). Note: TPM ≥1 is considered as "expressed". Voltage-gated Ca^{2+} channel subunits and directly associated channels are in **bold**, auxiliary/modulatory/regulatory subunits in *italics*. Human Protein Atlas version 16, Release date: 04.12.2016; Data retrieved on 10.01.2017.

#	Gene	a.k.a	adrenal gland	cerebral cortex	epididymis	esophagus	fallopian tube	heart muscle	kidney	lung	pancreas	parathyroid gland	prostate	skeletal muscle	skin	stomach	testis	TS	TPM	Gene description	Ensembl (ENSG00000…)
1	GRIN1	NMDAR1		■														202	152,3	Glutamate receptor, ionotropic, N-methyl D-aspartate 1	176884
2	*CATSPERD*	*TMEM146*															■	*160*	*15,9*	*Catsper channel auxiliary subunit delta*	*174898*
3	KCNJ1	Kir1.1							■									118	209,0	Potassium channel, inwardly rectifying subfamily J, member 1	151704
4	KCNJ9	Kir3.3		■														112	52,5	Potassium channel, inwardly rectifying subfamily J, member 9	162728
5	*CACNG7*			■														*101*	*63,9*	*Calcium channel, voltage-dependent, gamma subunit 7*	*105605*
6	GJA8	CX50															■	91	12,0	Gap junction protein, alpha 8, 50kDa	121634
7	AQP12A	AQP12									■							67	27,7	Aquaporin 12A	184945
8	CATSPER4																■	63	9,7	Cation channel, sperm associated 4	188782
9	GABRA1			■														44	109,1	Gamma-aminobutyric acid (GABA) A receptor, alpha 1	022355
10	KCNV2	Kv8.2															■	44	6,6	Potassium channel, voltage gated modifier subfamily V, member 2	168263
11	GABRA5			■														43	82,0	Gamma-aminobutyric acid (GABA) A receptor, alpha 5	186297
12	*CATSPERG*																■	*41*	*48,5*	*Catsper channel auxiliary subunit gamma*	*099338*
13	KCNA7	Kv1.7												■				37	26,2	Potassium channel, voltage gated shaker related subfamily A, member 7	104848
14	**CACNA1S**	**Cav1.1**												■				**34**	**103,0**	**Calcium channel, voltage-dependent, L type, alpha 1S subunit**	081248
15	*CACNG8*			■														*32*	*23,8*	*Calcium channel, voltage-dependent, gamma subunit 8*	*142408*
16	KCNF1	Kv5.1		■														32	37,6	Potassium channel, voltage gated modifier subfamily F, member 1	162975
17	CATSPER1	CATSPER															■	31	20,4	Cation channel, sperm associated 1	175294
18	**RYR1**													■				**30**	**572,4**	**Ryanodine receptor 1 (skeletal)**	196218
19	*CACNG3*			■														*28*	*42,6*	*Calcium channel, voltage-dependent, gamma subunit 3*	*006116*
20	CHRNE	ACHRE						■										27	34,4	Cholinergic receptor, nicotinic, epsilon (muscle)	108556
21	CATSPER3	CACRC															■	26	38,3	Cation channel, sperm associated 3	152705
22	***CACNG1***	***CACNLG***												■				***25***	***113,5***	***Calcium channel, voltage-dependent, gamma subunit 1***	*108878*
23	GRIN2B	NMDAR2B		■														25	13,2	Glutamate receptor, ionotropic, N-methyl D-aspartate 2B	273079
24	KCNU1	KCa5.1															■	24	13,4	Potassium channel, subfamily U, member 1	215262
25	*KCNE2*															■		*23*	*170,2*	*Potassium channel, voltage gated subfamily E regulatory beta subunit 2*	*159197*
26	KCNV1	Kv8.1		■														23	21,9	Potassium channel, voltage gated modifier subfamily V, member 1	164794
27	SCN2A	Nav1.2		■														22	58,5	Sodium channel, voltage gated, type II alpha subunit	136531
28	CHRNA2												■					20	43,0	Cholinergic receptor, nicotinic, alpha 2 (neuronal)	120903
29	CHRNG	ACHRG												■				19	8,2	Cholinergic receptor, nicotinic, gamma (muscle)	196811
30	SCN5A	Nav1.5						■										18	26,9	Sodium channel, voltage gated, type V alpha subunit	183873
31	CHRNA10													■				17	16,6	Cholinergic receptor, nicotinic, alpha 10 (neuronal)	129749
32	CLCN1	CLC1												■				17	22,9	Chloride channel, voltage-sensitive 1	188037
33	GABRG1			■														17	26,1	Gamma-aminobutyric acid (GABA) A receptor, gamma 1	163285
34	KCNK12	K2p12.1		■														16	5,3	Potassium channel, two pore domain subfamily K, member 12	184261
35	GABRB1			■														15	19,8	Gamma-aminobutyric acid (GABA) A receptor, beta 1	163288
36	CHRNB2			■														14	22,0	Cholinergic receptor, nicotinic, beta 2 (neuronal)	160716
37	CHRND	ACHRD												■				14	9,6	Cholinergic receptor, nicotinic, delta (muscle)	135902
38	KCNQ3	Kv7.3		■														14	26,9	Potassium channel, voltage gated KQT-like subfamily Q, member 3	184156
39	*CACNG2*	*stargazin*		■														*13*	*15,4*	*Calcium channel, voltage-dependent, gamma subunit 2*	*166862*
40	GABRA4			■														12	15,1	Gamma-aminobutyric acid (GABA) A receptor, alpha 4	109158
41	KCNH1	Kv10.1		■														12	11,5	Potassium channel, voltage gated eag related subfamily H, member 1	143473
42	KCNK4	K2p4.1		■														12	4,3	Potassium channel, two pore domain subfamily K, member 4	182450
43	GABRB2			■														11	63,0	Gamma-aminobutyric acid (GABA) A receptor, beta 2	145864
44	KCNC2	Kv3.2		■														11	46,5	Potassium channel, voltage gated Shaw related subfamily C, member 2	166006
45	*KCNRG*						■											*11*	*51,5*	*Potassium channel regulator*	*198553*
46	PKD2L2	TRPP5															■	11	15,6	Polycystic kidney disease 2-like 2	078795
47	SCN3B			■														11	132,5	Sodium channel, voltage gated, type III beta subunit	166257
48	*CNIH2*			■														*11*	*53,0*	*Cornichon family AMPA receptor auxiliary protein 2*	*174871*
49	*RAPSN*													■				*10*	*30,0*	*Receptor-associated protein of the synapse*	*165917*
50	ASIC1			■														10	57,0	Acid sensing (proton gated) ion channel 1	110881
51	GABRD			■														10	47,4	Gamma-aminobutyric acid (GABA) A receptor, delta	187730
52	GRIA4	GluA4		■														10	73,4	Glutamate receptor, ionotropic, AMPA 4	152578
53	GRID2	GluD2															■	10	59,7	Glutamate receptor, ionotropic, delta 2	152208
54	KCNN1	KCa2.1		■														10	21,5	Potassium channel, calcium activated subfamily N alpha, member 1	105642
55	GJB2	CX26				■												9	728,4	Gap junction protein, beta 2, 26kDa	165474
56	**RYR2**							■										**9**	**68,2**	**Ryanodine receptor 2 (cardiac)**	198626
57	GABRG2			■														9	74,3	Gamma-aminobutyric acid (GABA) A receptor, gamma 2	113327
58	ASIC4			■														8	10,6	Acid sensing (proton gated) ion channel family member 4	072182
59	GRIA2	GluA2		■														8	207,2	Glutamate receptor, ionotropic, AMPA 2	120251
60	KCNC1	Kv3.1		■														8	16,5	Potassium channel, voltage gated Shaw related subfamily C, member 1	129159
61	TRPM8												■					8	128,7	Transient receptor potential cation channel, subfamily M, member 8	144481

62	**CACNA1E**	**Cav2.3**		■														**7**	**10,3**	**Calcium channel, voltage-dependent, R type, alpha 1E subunit**	**198216**
63	CHRNA3		■															7	48,2	Cholinergic receptor, nicotinic, alpha 3 (neuronal)	080644
64	GABRA3			■														7	28,9	Gamma-aminobutyric acid (GABA) A receptor, alpha 3	011677
65	HCN1			■														7	11,5	Hyperpolarization activated cyclic nucleotide gated potassium channel 1	164588
66	KCNJ6	Kir3.2		■														7	2,6	Potassium channel, inwardly rectifying subfamily J, member 6	157542
67	KCNK7	K2p7.1													■			7	53,1	Potassium channel, two pore domain subfamily K, member 7	173338
68	KCNQ2	Kv7.2		■														7	56,3	Potassium channel, voltage gated KQT-like subfamily Q, member 2	075043
69	TRPM7											■						7	212,8	Transient receptor potential cation channel, subfamily M, member 7	092439
70	ANO3	TMEM16C			■													6	61,3	Anoctamin 3	134343
71	*BSND*								■									*6*	*10,2*	*Barttin CLCNK-type chloride channel accessory beta subunit*	*162399*
72	***CACNA2D2***									■								***6***	***73,0***	***Calcium channel, voltage-dependent, alpha 2/delta subunit 2***	*007402*
73	CHRNB3																■	6	3,7	Cholinergic receptor, nicotinic, beta 3 (neuronal)	147432
74	GABRA2			■														6	74,5	Gamma-aminobutyric acid (GABA) A receptor, alpha 2	151834
75	GABRR1																■	6	1,8	Gamma-aminobutyric acid (GABA) A receptor, rho 1	146276
76	GRIA1	GluA1		■														6	67,3	Glutamate receptor, ionotropic, AMPA 1	155511
77	GRIK3	GluK3		■														6	19,8	Glutamate receptor, ionotropic, kainate 3	163873
78	KCNA1	Kv1.1		■														6	13,5	Potassium channel, voltage gated shaker related subfamily A, member 1	111262
79	KCNH7	Kv11.3		■														6	4,7	Potassium channel, voltage gated eag related subfamily H, member 7	184611
80	SCN3A	Nav1.3		■														6	18,0	Sodium channel, voltage gated, type III alpha subunit	153253
81	SCN8A	Nav1.6		■														6	22,1	Sodium channel, voltage gated, type VIII alpha subunit	196876
82	GJB4	CX30.3													■			5	27,8	Gap junction protein, beta 4, 30.3kDa	189433
83	GRIN2A	NMDAR2A		■														5	25,0	Glutamate receptor, ionotropic, N-methyl D-aspartate 2A	183454
84	KCNA2	Kv1.2		■														5	20,7	Potassium channel, voltage gated shaker related subfamily A, member 2	177301
85	SCN2B			■														5	34,8	Sodium channel, voltage gated, type II beta subunit	149575

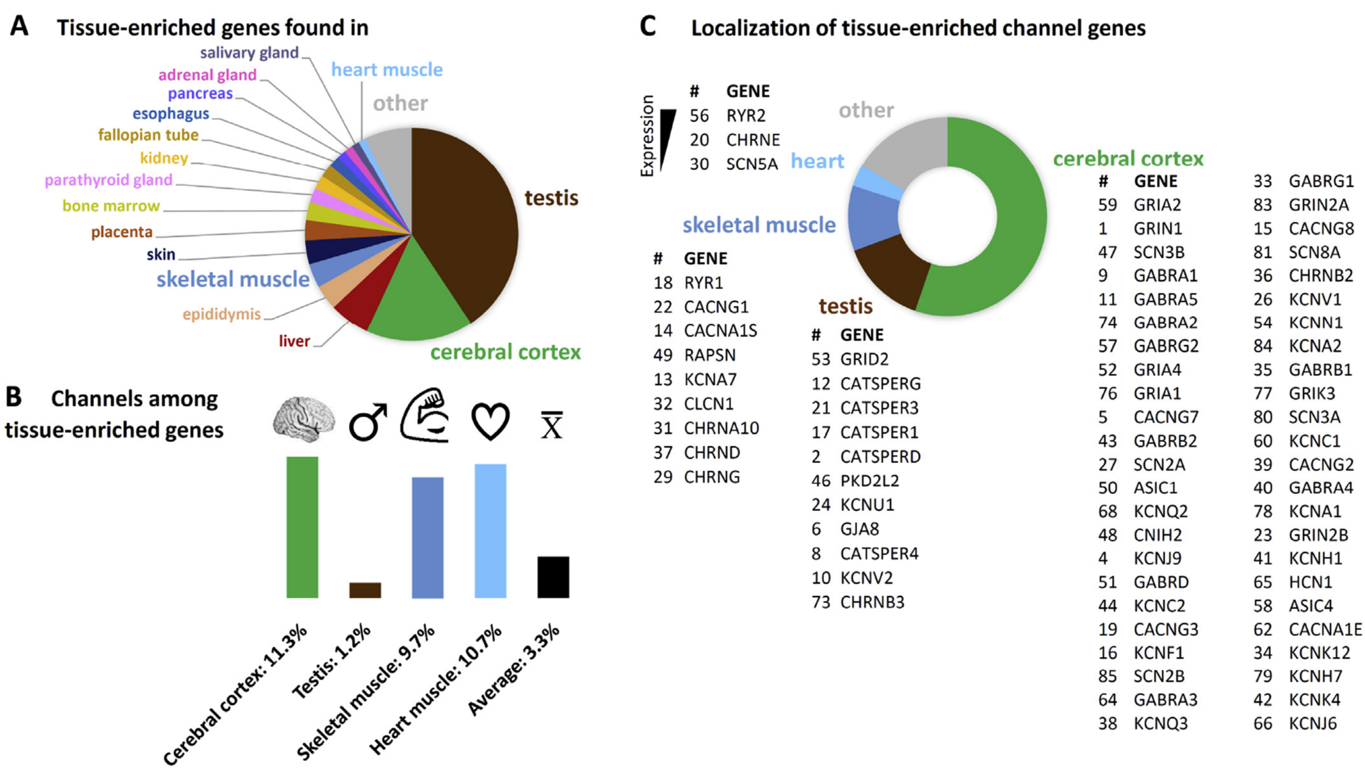

Fig. 1. Localization of all tissue-enriched genes and of the tissue-enriched channel genes.
(A) The largest number of tissue-enriched genes were found in testis (brown) and cerebral cortex (green) samples (tissue-enriched genes are defined by at least five-fold higher expression in one tissue compared to the tissue with the second highest expression. Only tissues with ≥1% of the total number of tissue-enriched genes are labelled. **(B)** Within each tissue, a different fraction of tissue-enriched genes belong to the ion channel families. While the electrically active tissues (cerebral cortex, skeletal (dark blue) and heart muscle (light blue)) have a higher-than-average percentage of channel genes, in testis only a low fraction of the tissue-enriched genes are channels. **(C)** Most tissue-enriched channels are found in cerebral cortex (green), testis (brown) and skeletal muscle (dark blue). Genes are listed in order of their expression strength (highest expression (TPM) on top). The numbering refers to Table 1. All data was taken from the Human Protein Atlas (retrieved from www.proteinatlas.org on 11.01.2017).

2016). Among auxiliary subunits, all β subunits as well as $\alpha_2\delta$-2 have been described in immune cells (Robert et al., 2014; Jha et al., 2015; Cabral et al., 2010), which conforms to FANTOM5 lymphoid tissue data.

Moreover we compared expression data of the human retina with mouse retina quantitative RT-PCR data from Knoflach et al. (2013) (Fig. 2E). To this end we normalized all expression values to the highest expressed gene, $\alpha_2\delta$-4. While the quantitative expression values differed, the qualitative relationships between different VGCC subunits within each species were conserved. In

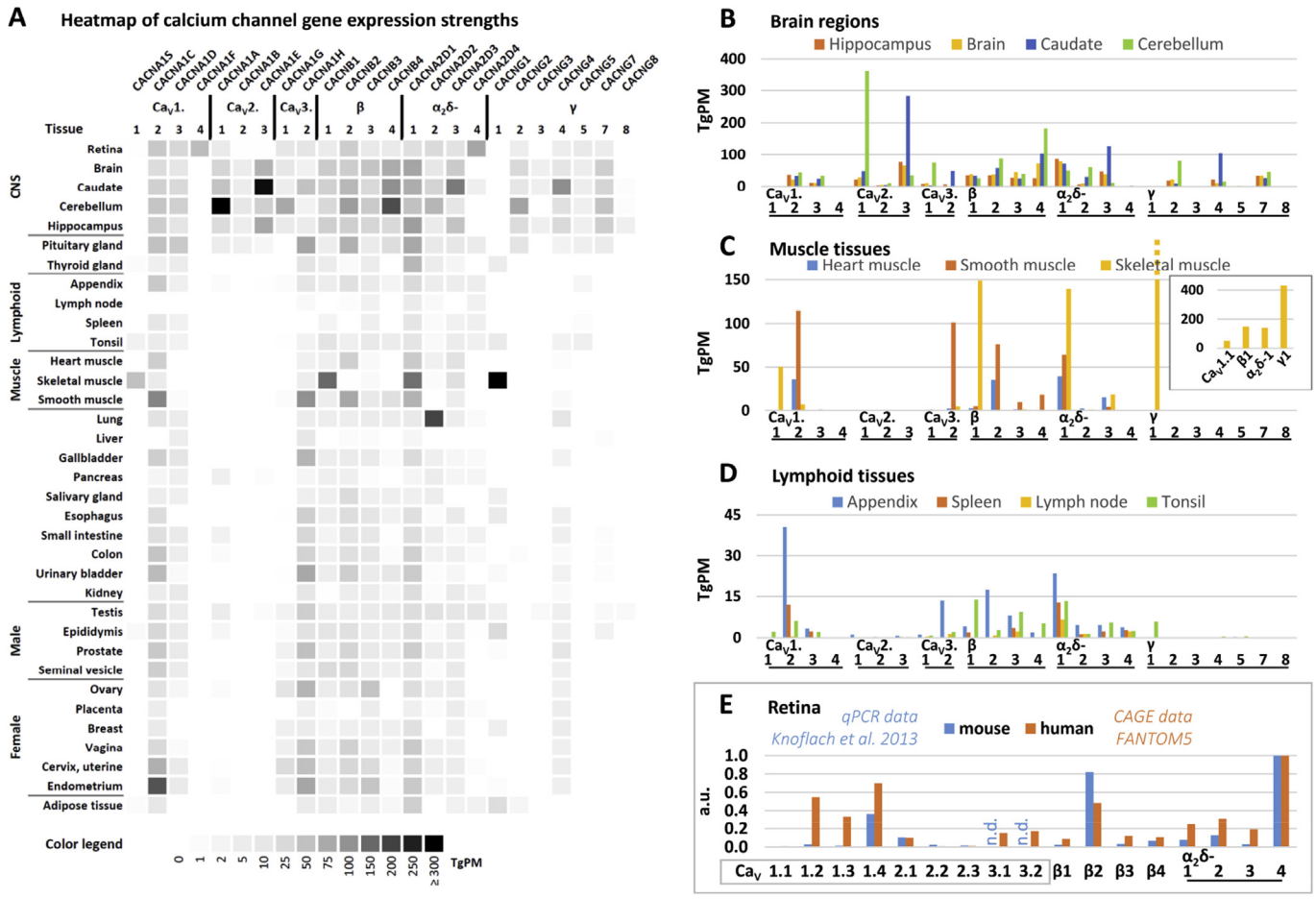

Fig. 2. VGCC gene expression in different human tissues and mouse retina.
(A) Heatmap of VGCC gene expression strengths across tissues. Darker hues indicate higher expression (TgPM = tags per million). Because the HPA dataset contained only a part of the brain (cerebral cortex) and no retinal samples, we chose FANTOM5 data for this comparison which were shown to highly correlate with the HPA (Yu et al., 2015b). Note that $Ca_V3.3$ and γ_6 data was not available from FANTOM5 and using another database for the comparison of absolute values was not possible. **(B)** Expression of VGCCs in different brain regions. Note that "Brain" is a whole-brain sample. **(C)** Expression of VGCCs in muscle tissue. The inset shows the skeletal muscle calcium channel subunit encoding genes. Note the high abundance of $\gamma 1$. **(D)** Expression of VGCCs in lymphoid tissues **(E)** Comparison of expression of VGCC in mouse and human retina. Data were normalized to $\alpha_2\delta$-4. FANTOM5 data was retrieved through Human Protein Atlas website www.proteinatlas.org on 11.01.2017. VGCC nomenclature according to Catterall et al. (2005).

both mouse and human retinas $Ca_V1.4$ was the most abundantly expressed pore-forming $\alpha 1$ subunit, $Ca_V2.1$ the most abundant Ca_V2 member and β_2 was the main β subunit. The outcome for Cav1.4 and β2 is compelling confirming the suitability of mouse models for investigations in human Cav1.4 related channelopathies (see also below; (Zeitz et al., 2015)). The major difference between the two datasets lies in the high expression values for $Ca_V1.2$ and $Ca_V1.3$ in the human retina data. Most likely this can be explained by abundant RNA from retinal pigment epithelium (RPE) in the samples used for FANTOM5, which is evident in the high expression values of RPE-specific genes (e.g. PMEL, RGR, RPE65) in the retina data set (not shown). In fact, both $Ca_V1.2$ and $Ca_V1.3$ have been found prominently in RPE (Wimmers et al., 2008; Muller et al., 2014).

Fig. 3 takes a look at the FANTOM5 expression data from the other angle: Which tissues express a given VGCC gene. It is immediately obvious that $Ca_V1.1$ and $Ca_V1.4$ have very restricted expression mostly in a single tissue, while $Ca_V1.2$ and $Ca_V1.3$ were found in a large number of different tissues. All three Ca_V2 channel isoforms were detected almost exclusively in different parts of the brain, where also β_4, $\alpha_2\delta$-3 and $Ca_V3.3$, to a smaller degree, $Ca_V3.1$ were more prominently found. Most of the γ subunits were also mainly localized in the CNS. Other tissue-elevated expression profiles included β_1, $\gamma 1$, $\gamma 6$ (skeletal muscle), $\alpha_2\delta$-2 (lung) and $\alpha_2\delta$-4 (retina).

While FANTOM5 data is largely ignorant of alternative splicing (except 5′ transcription start sites), the HPA data set can also be used to check for the expression of (Ensembl-annotated) splice variants. As an example the two Cav1.1 splice variants, one 'full-length' and Cav1.1Δ29 (Ensembl identifiers ENST00000362061, ENST00000367338; see also chapter 4) have a slightly different expression distribution. While in skeletal muscle samples the 'full-length' Cav1.1 is ~5-fold more abundant than Cav1.1Δ29, it seems to dominate in esophagus.

Some caveats of these databases have to be kept in mind: on one hand only tissues that have been sampled can be compared, on the other hand tissues can be heterogeneous and therefore have a very different channel set in different parts of the organ. This was obvious from the Cav1.4 expression in the HPA data where it is deemed non-specific because there is no retina sample included. Moreover contributions from retina and retinal pigment epithelium could not be distinguished in the FANTOM 5 dataset because presumably these two tissues were not separated during the sample preparation. In general, both the subunit composition of multimeric channels as well as other interactions can affect the severity

Table 2
Expression of VGCC α1 subunit splice variants. Both tissue source and species are indicated. Existing channelopathies or specific interactions with drugs are indicated in bold (disease) or italic (pharmacology). Abbreviation: n.i., not indicated.

α1 subunit	Splice variant	Tissue expression	Species	Disease *pharmacology*	Reference PMID
Cav1.1	Δ exon 29	spleen (CD4 T cells)	mouse		26815481
	Δ exon 29	muscle biopsy	human	**Myotonic dystrophy type 1 and type 2**	23888875
	Δ exon 29	muscle biopsy	human	**Myotonic dystrophy type 1 and type 2**	22140091
	Δ exon 29	muscle, primary myotubes, C2C12 line	Human mouse		19134469
Cav1.2	$Cav1.2_{e21+22}$	heart	mouse	**Cardiac hypertrophy, heart failure**	27731386
	$Cav1.2_{33L}$	heart (neonatal, adult)	mouse		25694430
	1896G>A	n.i.	human	**Brugada syndrome**	24321233
	$Cav1.2_{\Delta 73}$	cardiovascular tissue	human		23926129
		brain, A7r5 cells	rat		
	$Cav1.2_{\Delta 9^*}$	aorta cDNA library	human		21998324
	exons 8, 8a	cortex	mouse	**Timothy Syndrome**	21282112
	exons 8/8a, 9, 33	cardiac and smooth muscle	n.i.	*Diltiazem sensitivity*	20649567
	exon 9*	cerebral artery myocytes	rabbit		19717733
	exons 9*, 33	embryonic cortex	mouse		19564422
	exons 9*, 33	heart	rat	**Myocardial infarction rat model**	19263075
	exons 1a, 1, 8a, 8, 9*, 21, 22, 31, 32, 32-6nt, 33	heart	rat	**Hypertensive rat model**	18070605
	exons 8/8a, 9, 33	cardiac and smooth muscle		*Nifedipine sensitivity*	17916557
	exon 9*	cartilage, bone, fat, liver, kidney, aorta, bladder, heart tissues, CNS	human		15916803
	exon 9*	smooth muscle	rat		15381693
	exons 21, 22	brain	rat	*Isradipine sensitivity*	7737988
	α1C-a	heart	rat	*Nisoldipine sensitivity*	9314833
	α1C-b	aorta			
	exons 8, 8a, 31, 32, 40–43	n.i.	human	*Isradipine sensitivity*	9607315
Cav1.3	exons 42S, 42L, 43S, 43L	whole-brain, brain regions, inner ear, sinoatrial node	human		26379493
			mouse		21998310
	C-terminus	testis, heart, pancreas, kidney, lung	hamster		21093409
	exon 43S	whole-brain, brain regions, heart, eye	human		21998310
			mouse		
	exons 42, 42S 43S, Δ41, Δ44, 48S	whole-brain, brain regions, spinal cord	mouse		21998309
	exons 42, 42A	whole brain, brain regions	human		18482979
	$Cav1.3_b$	cortical neuron culture	rat		17287512
	$Cav1.3_{\Delta IQ}$	cochlea inner hair cell	rat		17050708
	$Cav1.3_a$	striatal medium spiny neurons	mouse		15689540
	$Cav1.3_b$				
	$Ca_v1.3_{1a}$	$Ca_v1.2^{-/-}$ cardiomyocyte	mouse		12900400
	$Ca_v1.3_{1b}$				
	$Cav1.3_{short}$	neuroendocrine cells, whole-brain, pituitary GH3 cells	rat		11514547
	exons 31, 32	ventricular myocytes	human	**Heart failure**	10888251
	IIIS2	cochlea	chicken		9405709
	26 ins $_{I-II}$				
	10 ins $_{IVS2-S3}$				
	IVS3-IVS4	whole-brain, heart, lung, aorta	rat		9405178
	rCACN4A, 4B, C-terminus, I-II loop, IVS3-S4	RINm5F cell line	rat		7760845
Cav1.4	Δ exon 45,	retina	human		27226626
	Δ exon 47,		monkey		
	Δ exon p45,47		mouse		
	transcript scanning	retina Marathon®-Ready cDNA	human		22069316
	$Ca_V1.4a$, b	Jurkat T cells, peripheral blood T	human		15899519
	exons 31–34, 37	lymphocytes, activated T cells			
Cav2.1	C-terminus	neurosecretory cells			24344901
	exons 46, 47	n.i.		**Spinocerebellar ataxia type 6**	21550405
	splicing mutations	blood samples	human	**Episodic ataxia type 2**	20129625
	Δ exon 47	n.i.	n.i.	**Familial hemiplegic migraine type 1**	19242091
	Δ synprint	neuroendocrine cells	rat		18390553
	Δ exon1	whole-brain, cultured cells			
	Δ exon 2				
	exon 47 ins	Purkinje and granule cells	human	**Spinocerebellar ataxia type 6**	18835329
			patient		
	exons 37a, 37b	whole-brain, cerebellum	mouse		17291689
			rat		
	exons 28, 34, 47	cerebellum, Purkinje neurons	rat		16278278
	α1A-a, α1A-b	brain regions	rat		10321243
Cav2.2	exons 18a, 24a, 31a, 37a, 37b	whole-brain, cerebellum	mouse		21150296
		dorsal root ganglion			
	exons 37a, 37b	n.i.	mouse	*Analgesic treatment*	24369063
	exon 37a	dorsal root ganglia	mouse		22836269
	exon 18a ins	hippocampus,	rat	**Chronic inflammatory pain**	19125229
	Δ exon 1	spinal cord			

(*continued on next page*)

Table 2 (*continued*)

α1 subunit	Splice variant	Tissue expression	Species	Disease *pharmacology*	Reference PMID
	exons 18a, 24a, 31a, 37a, 37b	dorsal root ganglia	rat		14715140
	Δ exon 1 Δ exon 2	fetal and adult brain	human		11756491
	II–III loop	superior cervical and dorsal root ganglia, spinal cord, brain regions	rat		10864934
	synprint II-III loop	ventral mesencephalon	rat		10501220
	IIIS3-S4 IVS3-S4	whole-brain, superior cervical ganglia	rat		9010213
	$\alpha 1E_{-L}$	retina, brain regions	rat		9582423
Cav3.1	transcript scanning Δ exon 14 Δ exon26	whole-brain, thalamus, cortex, cerebellum, hippocampus	mouse	**Absence epilepsy (lethargic, tottering)**	19480703
	exons 25, 26	dorsal thalamus	rat		17707654
	exons 14, 25, 26, 34, 35, 38B	infant brain	human		10548410
Cav3.2	± exon 25	heart tissues		**Hypertension- associated cardiac hypertrophy**	20699644
Cav3.3	exons 33, 34	brain regions, pineal gland	rat		12297319

of channel dysfunctions. Co-expression in a tissue or even a cell-type does not yet prove a functional interaction, but these catalogues can help to identify common candidates for protein interaction networks or even new players, including also non-channel proteins.

3. Tissue specific expression of L-type Ca^{2+} channels

We found a great heterogeneity in the tissue expression of LTCC isoforms. This diversity is expected to impact also on different functional roles of LTCCs in the different tissues. Indeed their physiological importance reaches from excitation-contraction coupling in muscle, to stimulus secretion coupling in sensory and endocrine cells, cardiac pace-making, as well as neuronal firing to learning and memory (Catterall et al., 2005). Cav1.2 and Cav1.3 channels are both expressed in heart, brain, endocrine cells, and auditory and vestibular receptor cells (for review see (Zamponi et al., 2015)). In some neurons, adrenal chromaffin cells, sinoatrial node and atrial cardiomyocytes those isoforms are often even expressed in the same cell type (Olson et al., 2005; Chan et al., 2007; Dragicevic et al., 2014; Marcantoni et al.; Mangoni et al., 2003). Their differential contribution to cellular processes and their physiological functions can therefore only be distinguished in Cav1.2- and Cav1.3-deficient animals (for reviews on animal models see (Striessnig and Koschak, 2008; Hofmann et al., 2014). Cav1.1 and Cav1.4 α1 transcripts were not found at significant levels in the brain (Figs. 2B and 3; Sinnegger-Brauns et al., 2009). Expression in a limited subset of (brain) neurons or - with respect to Cav1.4 mRNA expression - contamination with pineal gland tissue where Cav1.4 has been reported to be expressed (McRory et al., 2004; Yu et al., 2015a) can't however be entirely excluded. Of note, immunohistochemical analyses that previously reported expression of Cav1.1 in retinal tissue (Specht et al., 2009; Michalakis et al., 2014; Tummala et al., 2014) were carried out with a Cav1.1-directed antibody that was recently discovered to cross-react with GPR179 (Hasan et al., 2016). Additional western blot and mass spectrometric analyses of Cav1.1 immunoprecipitated proteins also failed to detect any matching Cav1.1 peptides, however a novel splice variant with exons 1–16 skipped and two novel exons termed 16a and 16b has been found by RNAseq (Hasan et al., 2016).

Being described as an atypical prototypical VGCC Cav1.1 is expressed solely in skeletal muscle where it serves as voltage sensor for excitation-contraction coupling and contributes excitation-coupled Ca^{2+} entry (for review see (Bannister and Beam, 2013)). In skeletal muscle Cav1.1 is located within the junctional membranes of the t-tubule system where it physically interacts with ryanodine-sensitive release channels in the sarcoplasmic reticulum in order to trigger rapid Ca^{2+} release and mediated muscle contraction. Cav1.4 expression however is primarily restricted to the retina. Cav1.4 immunoreactivity has been first described in the outer and inner plexiform layers of chicken retina (Firth et al., 2001). Its expression at photoreceptor release sites located in close vicinity to the typical horseshoe-shaped ribbon synapses has been confirmed in many studies on rodent and zebrafish retina (Mansergh et al., 2005; Specht et al., 2009; Liu et al., 2013; Knoflach et al., 2013; Michalakis et al., 2014; Regus-Leidig et al., 2014; Jia et al., 2014; An et al., 2015; Grabner et al., 2015). Cav1.4 expression in retinal bipolar cells has also been suggested (Berntson et al., 2003; Busquet et al., 2010; Morgans et al., 2005) but functional assessment of the channel subunit composition is lacking. The LTCC identity of these neurons is therefore still ambiguous. As already mentioned above, Cav1.4 was further detected outside the retina in mouse, including tissue of the immune system and the pineal gland (McRory et al., 2004; Kotturi and Jefferies, 2005; Yu et al., 2015a).

4. L-type Ca^{2+} channel diversity by alternative splicing and its consequences

As the reader can take from Table 2, literature about the post-transcriptional mechanism of alternative splicing in VGCCs is rapidly emerging as is the information about the functional heterogeneity encoded by those alternatively spliced gene products. Alternative splicing is important in all four α1 isoforms of LTCC. For example one Cav1.1 variant that differs in the length of the IVS3-S4 linker due to skipping of exon 29 (Cav1.1Δ29, see also Table 2) was abundantly expressed in mouse and human myotubes (Tuluc et al., 2009) and has also been reported in mouse spleen (Matza et al., 2016). Of note, muscle weakness in the pathogenesis of human myotonic dystrophy type 1 (DM1) and type 2 (DM2) has been related to the aberrant Cav1.1 splicing and altered gating properties in the resulting Cav1.1Δ29 channels (Tang et al., 2012; Santoro et al., 2014).

A rodent splice variant of Cav1.2 that contained the mutually exclusive exons 21 and 22 ($Cav1.2_{e21+22}$) resulted in non-conducting Cav1.2 channels. In heterologously transfected HEK-293 cells $Cav1.2_{e21+22}$ in turn reduced the number of cell surface

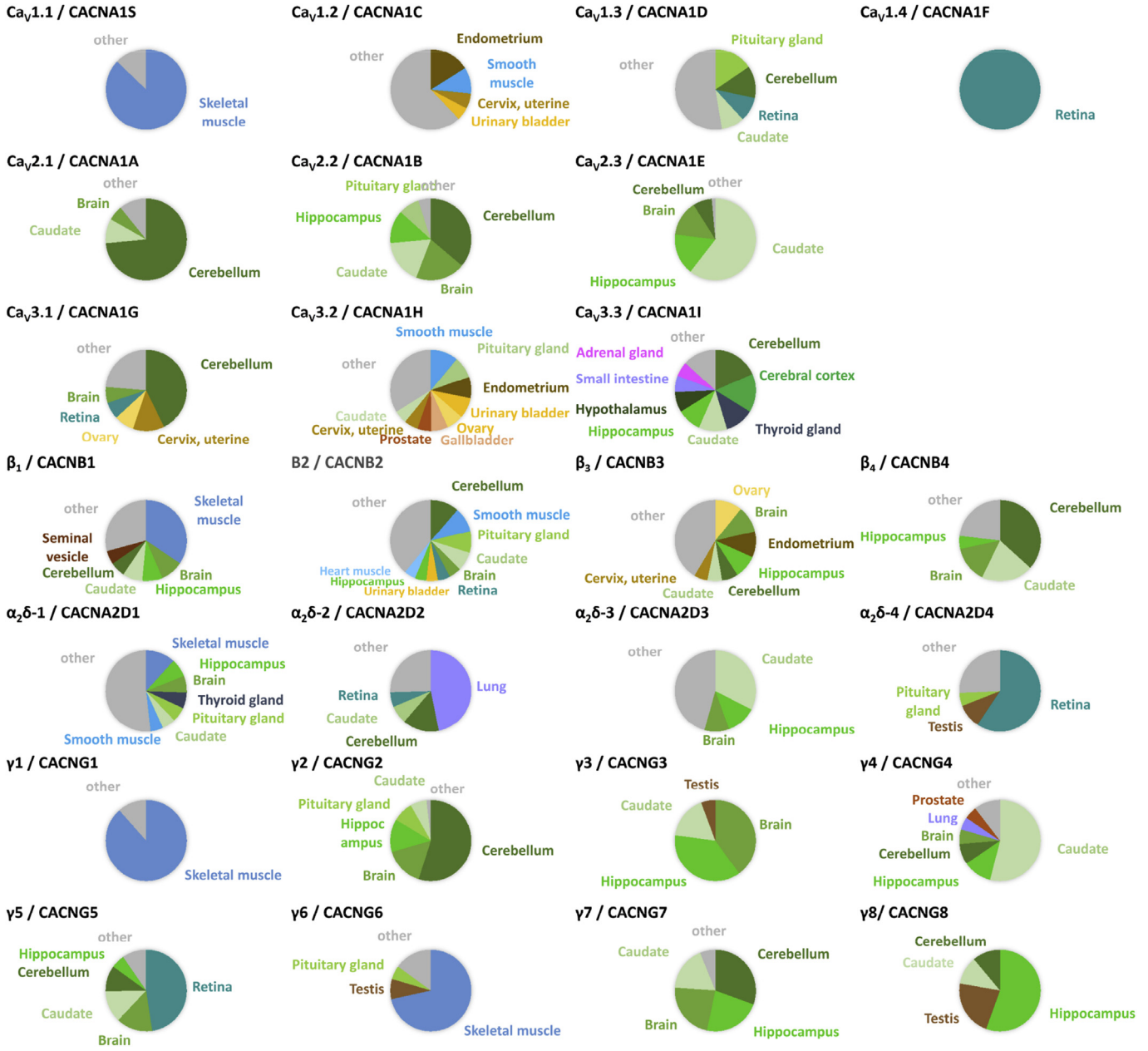

Fig. 3. Distribution of VGCC gene expression in human tissues.
Tissues names are given where the expression exceeds 5% of the total expression in all tissues (except for β_2: retina: 4.9%, heart 4.6%). The colour code is the same throughout: brain tissues (green hues), muscle tissues (blue hues), other tissues are indicated by different colours. Less expressed tissues are combined as 'others' (grey). Some of the VGCC genes show highly abundant expression (>50% of total): $Ca_V1.1$, $Ca_V1.4$, $Ca_V2.1$, $Ca_V2.3$, $\alpha_2\delta$-4, γ_1, γ_2, γ_4, γ_6, γ_8. Others are particularly expressed in several brain areas (together >50% of total): $Ca_V2.2$, $Ca_V3.1$, β_4, $\alpha_2\delta$-3, γ_3, γ_7. Some are expressed preferentially (>33% of total): β_1, $\alpha_2\delta$-2, γ_5. The remaining genes showed widespread expression: $Ca_V1.2$, $Ca_V1.3$, $Ca_V3.2$, β_2, β_3, $\alpha_2\delta$-1. According to the tissue specificity score (TS) calculation of the Human Protein Atlas (highest expression/2nd highest expression), the tissue-enriched VGCC are (TS score): $Ca_V1.4$ (∞), $Ca_V1.1$ (22.8), γ_1 (21.0), γ_6 (9.0), $Ca_V2.1$ (7.6) and $\alpha_2\delta$-4 (6.2). Note that $Ca_V3.3$ and γ_6 expression data stems from the GTEx dataset (no FANTOM5 data available on HPA website). FANTOM5 data was retrieved through www.proteinatlas.org on 11.01.2017, GTEx on 12.06.2017).

expressed wild type Cav1.2 channels by enhanced ubiquitination and subsequent proteasomal degradation, that consequently also decreased Cav1.2 mediated Ca^{2+} influx (Hu et al., 2016). This variant was highly expressed in the neonatal heart but no expression in brain was reported. Under stressful conditions also adult mouse and human hearts showed increased abundance indicating that this splice variant may even contribute to heart failure (Hu et al., 2016). Another study showed that in a rat myocardial infarction model the expression of a number of alternatively spliced exons were changed. Upon ligation of a descending artery a novel Cav1.2 9*/delta33 channel (inclusion of exon 9* and deletion of exon 33) was generated in the scar region that exhibited hyperpolarized shifts of the voltage-dependence of activation and inactivation in the heterologous expression system (Liao et al., 2009). Intriguingly, in Cav1.2 the binding site for DHPs - which specifically block LTCCs – is encoded by the exclusive exons 8 and 8a (see also Table 2). Cav1.2 channels containing exon 8 are expressed in smooth muscle and display a 10-fold greater affinity for DHP blockers than exon 8a containing channels which comprise the cardiac form (Welling et al., 1997). However, in human heart tissue samples - taken

from heart transplant recipients - a subset of tissues expressed predominantly the exon 8 containing smooth muscle isoform, rather than the cardiac isoform (Welling et al., 1997; Wang et al., 2006). This finding suggested that in affected individuals therapeutic DHP treatment could cause strong unwanted effects in the heart. This is a clear example highlighting that interindividual variability in alternative splicing can severely modulate pharmacological effects through distinct tissue expression and therefore cause harm to patients.

Furthermore, also drug action on Cav1.3 channels depends on the effects of alternative splicing. An intramolecular interaction between a distal and a proximal regulatory domain – forming an intrinsic C-terminal modulatory mechanism, short CTM - within the Cav1.3 C-terminus is a major determinant of their voltage- and Ca^{2+}-dependent gating kinetics (Striessnig, 2007). Splicing in the C-terminus of Cav1.3 α1 subunits gives rise to fundamentally different channels with either 'long' or 'short' C-termini. Thereby removal of the CTM domains by alternative splicing generates the 'short' Cav1.3 ($Cav1.3_{42A}$, $Cav1.3_{43S}$) channels. These splice isoforms activated at a more negative voltage range and exhibited different voltage- and Ca^{2+}-dependent inactivation properties of these channels (Bock et al., 2011; Singh et al., 2008; Tan et al., 2012). At this point it is important to know that the action of DHPs depends on the inactivated channel state (Bean et al., 1986; Hamilton et al., 1987; Koschak et al., 2001; Berjukow and Hering, 2001) such that DHPs possess a higher affinity for the inactivated channel conformation. The amount of channel block is therefore expected to change with the availability of inactivated channel states. Of note, the expression of both short and long variants showed a certain tissue specificity. The long variant seemed to predominate in the heart whereas expression of both variants were about equally abundant in the brain (Bock et al., 2011). Together, this suggests that DHP drugs might act differently on Cav1.3 channel variants expressed in different tissues to fine-tune channel function (Huang et al., 2014; Ortner et al., 2017). Also in Cav1.4, the most abundantly expressed LTCC in the retina, alternative splicing occurs. In a transcript scanning approach of human retina samples, 19 Cav1.4 splice variants were identified (Tan et al., 2012). One of those also resulted in a truncation of the channels' C-terminus ($Ca_V1.4$ ex43*). Similar to Cav1.3 channels, such structural change is also expected to severely affect the voltage- and Ca^{2+}-dependent gating properties of Cav1.4 channels (Singh et al., 2006; Wahl-Schott et al., 2006). Indeed, the loss of CTM in the splice variant $Ca_V1.4$ ex43* resulted in robust Ca^{2+}-dependent inactivation and a hyperpolarized activation range (Haeseleer et al., 2016). Such gating changes might be even pathological for visual signaling (Singh et al., 2006; Wahl-Schott et al., 2006). Though a recent heterologous expression study provided evidence that coexpression of CaBP4 - a member of a family of Ca^{2+}-binding proteins (CaBPs) related to CaM and expressed in retinal photoreceptors (Haeseleer et al., 2004) – could at least in part compensate for the expected Cav1.4 gating changes by binding to the remaining C-terminal domain of the $Ca_V1.4$ C-terminus (Haeseleer et al., 2016). To which extent these naturally occurring alternative splice variants indeed add to the properties of native Cav1.4 currents (von Gersdorff and Matthews, 1996; Rabl and Thoreson, 2002) or whether the abundance of particular splice variants is changed under pathophysiological conditions - as seen for all other LTCCs (Table 2) - is not yet resolved. Details on these functionally different Cav1.4 splice variants in other tissues (lymphocytes or pineal gland) are yet to be elucidated.

5. Manifestation of Cav1.4-related channelopathies and treatment challenges

Tissue expression of a certain protein often correlates with histological and functional features seen in animal models and humans as well as the clinical features in case of a dysfunctional protein. Among the LTCC family Cav1.4 is one of the finest examples.

The role of Cav1.4 is well supported by the fact that mutations in the *CACNA1F* gene can cause several forms of human retinal diseases (OMIM #300071, #300476, #300600, for review see (Zeitz et al., 2015)). The majority of Cav1.4 mutations were identified in congenital stationary night blindness type 2 (CSNB2) patients who are presenting with typical symptoms like low visual acuity, myopia, nystagmus, strabismus, photophobia and variable levels of night blindness (Bech-Hansen et al., 1998a,b). CSNB2 mainly involves males due to the X-linked nature of the disease but recent reports substantiated that heterozygote females can also be affected (Hope et al., 2005; Michalakis et al., 2014). Both loss of channel function and increased channel activity can lead to alterations in photoreceptor synapse formation. This has been demonstrated in Cav1.4 deficient mice ($Cav1.4^{-/-}$; (Morgans et al., 2001; Mansergh et al., 2005; Raven et al., 2008; Zabouri and Haverkamp, 2013; Specht et al., 2009)) and also in Cav1.4 mutant mice. The latter contain a point mutation at position Ile756Thr (corresponding to Ile745Thr in the patients) that induced enhanced channel activity obvious from a strong hyperpolarizing shift in the voltage-dependence of activation and slowing of the inactivation properties (Cav1.4-IT; (Hemara-Wahanui et al., 2005)). A large body of work done by many labs highlighted that Cav1.4 channels are central for the proper formation and maturation of photoreceptor synapses (Morgans et al., 2001; Mansergh et al., 2005; Chang et al., 2006; Bayley and Morgans, 2007; Raven et al., 2008; Zabouri and Haverkamp, 2013; Specht et al., 2009; Liu et al., 2013; Regus-Leidig et al., 2014; Michalakis et al., 2014).

Functional data from CSNB2 patients still implied an incomplete defect of the ON and OFF bipolar cells or their synapses in the rod and cone visual pathways (Miyake et al., 1986; Miyake, 2002). Indeed signal transmission was not completely blocked but some reduced activity remained in Cav1.4 mutant retinas (Chang et al., 2006; Knoflach et al., 2015). In the Cav1.4-IT mouse model the left shift in the voltage-dependence of channel activation was hypothesized to reduce the dynamic range of photoreceptor activity. In line with this hypothesis only a fraction of Cav1.4-IT ganglion cells responded to light stimulation in multielectrode array recordings from whole-mounted retinas, and spatial responses as well as changes in their contrast sensitivity profile were decreased in these mutants (Knoflach et al., 2015). Of note, strongly reduced visual acuity in fact turned out to be a major complaint in CSNB2 patients (Bijveld et al., 2013) and patients carrying the respective Cav1.4 mutation also showed pronounced vision loss (up to 80% (Hope et al., 2005)).

When we consider treatment of retinal Cav1.4-related channelopathies we face several challenges. The very restricted expression of Cav1.4 channels in retinal tissue should be a clear advantage for Cav1.4 targeted therapy. But still, in systemic pharmacotherapy due to the expression of Cav1.4 in immune cells or pineal gland tissue (see above) the potential effects on the immune system or the sleep/wake cycle would have to be controlled for, even though no obvious deficits in circadian rhythm or immune system have been documented so far in CSNB2 patients. The main problem however lies in the specificity of available drugs. Currently all LTCC blockers that are in clinical use, as for example the DHP nifedipine or other DHPs (Striessnig et al., 2015), are considered non-selective because Cav1.2, Cav1.3 and Cav1.4 channels only slightly differ in their DHP sensitivity (Koschak et al., 2001; Xu and Lipscombe, 2001; Koschak et al., 2003). Due to their high binding affinity to $Ca_V1.2$ channels DHPs mainly have cardiovascular effects ($Ca_V1.2$ expression in cardiovascular tissue, see Figs. 2C and 3; (Moosmang et al., 2003;

Zhang et al., 2006)). For this reason, DHPs are not applicable in CSNB2 patients – and also for treatment of other CNS disorders – considering the severe side effects of the necessary therapeutic doses (for review see (Zamponi et al., 2015)). When considering restoration of channel function either by pharmacological chaperoning in the retina (http://clinicaltrials.gov/ct2/show/study/NCT01233609) or gene-based retinal therapies.

(Sengillo et al., 2017), treatments likely would have to start early during retinal development because of the crucial role of Cav1.4 for proper synapse formation already mentioned above.

6. Gene therapy of Cav1.4 channelopathies

Treatment e.g. of skeletal muscle by gene therapy is considered in humans (for review (Saada et al., 2016; Sommese et al., 2017)) and has been demonstrated in animal models (Gruntman et al., 2013; Qiao et al., 2011) (Wang et al., 2014) even without the use of viral vectors (Lu et al., 2003), though the necessary systemic approach to treat all muscles in the body bears certain risks given by the widespread distribution of muscle tissues. The focal expression of Cav1.4 in the eye on the other hand provides a number of advantages which are briefly outlined in the following.

The eye is not only easily accessible but it is also a small sized and confined organ. Thus, low amounts of viral vectors are sufficient and there is little risk of a systemic spread of the vector. For this reason and for reasons explained below, the eye has been targeted in gene therapy (Sengillo et al., 2017; Scholl et al., 2016). In particular, intravitreal injections of vectors are easy to perform and constitute a routine procedure in eye hospitals without the need for inpatient admission. Intravitreal injections can reach large areas of the retina (Da Costa et al., 2016), a clear advantage over subretinal delivery, where a needle has to penetrate the retina to inject vectors between retina and choroid. Of note, adeno-associated viruses (AAV) that effectively target photoreceptors even from intravitreal injections (e.g. AAV.7m8) have been developed and applied successfully in gene therapy in mice (Dalkara et al., 2013). Alternatively, the functionality of selective promotors for expression in rods (Koch et al., 2012) or (S-)cones (Michalakis et al., 2010) without cell-type specific tropism has been demonstrated. Targeting other cell types is also feasible due to the comparatively well-known cell types in the retina and the knowledge about cell-type specific genes (Siegert et al., 2012) and promoters (Ivanova et al., 2010). In the case of Cav1.4 it might be necessary to treat not only photoreceptors but also bipolar cells that express Cav1.4 (Berntson et al., 2003), so a mixed approach of different vectors/tropisms or promotors could be required. Targeting Cav1.4 might still be challenging due to the size of the *CACNA1F* gene (OMIM 300100) and the limited packaging capacity of AAVs. However, split-intein-mediated protein transsplicing methods have already been used successfully to manipulate other LTCCs (Subramanyam et al., 2013).

Viral vector-based gene therapy benefits from the immune-privileged status and the specific location of the retina in the eye. The blood-retina barrier provides an advantage in the protection of treated cells from the patients' immune responses by limiting potential inflammatory reactions (Bennett, 2003). It has however been observed that intravitreal injections can trigger an immune response not observed by subretinal injections (Li et al., 2008). Still, the enclosed structure of the eye in conjunction with the blood-retina barrier provides a spatial restriction of gene therapeutic treatments almost unrivalled by other organs. These features are relevant for all genetic interventions, in particular in CRISPR/Cas9 applications (Hung et al., 2016; Latella et al., 2016; Bakondi et al., 2016; Yanik et al., 2017; Ruan et al., 2017) where off-target effects might not be fully excluded (Fu et al., 2014). Together, the eye/retina provides a high level of containment with limited immune response, making applications comparatively safe. Indeed several clinical trials of gene therapy for eye diseases in patients have been undertaken in recent years (Bainbridge et al., 2008; Maguire et al., 2008; Cideciyan et al., 2008). Cav1.4 mutations would therefore be amenable for gene therapeutic treatments in the foreseeable future.

Funding

This project has received funding from the European Union's Horizon 2020 research and innovation programme under the Marie Sklodowska-Curie grant agreement No 674901 to AK, and was supported by the Austrian Science Fund (FWF P-26881-B23, P-29359 to AK), the Center of Molecular Biosciences Innsbruck and the University of Innsbruck.

References

An, J., Zhang, L., Jiao, B., Lu, F., Xia, F., Yu, Z., Zhang, Z., 2015. Cacna1f gene decreased contractility of skeletal muscle in rat model with congenital stationary night blindness. Gene 562, 210–219.

Badou, A., Jha, M.K., Matza, D., Flavell, R.A., 2013. Emerging roles of L-type voltage-gated and other calcium channels in T lymphocytes. Front. Immunol. 4, 243.

Bainbridge, J.W., Smith, A.J., Barker, S.S., Robbie, S., Henderson, R., Balaggan, K., Viswanathan, A., Holder, G.E., Stockman, A., Tyler, N., Petersen-Jones, S., Bhattacharya, S.S., Thrasher, A.J., Fitzke, F.W., Carter, B.J., Rubin, G.S., Moore, A.T., Ali, R.R., 2008. Effect of gene therapy on visual function in Leber's congenital amaurosis. N. Engl. J. Med. 358, 2231–2239.

Bakondi, B., Lv, W., Lu, B., Jones, M.K., Tsai, Y., Kim, K.J., Levy, R., Akhtar, A.A., Breunig, J.J., Svendsen, C.N., Wang, S., 2016. In Vivo CRISPR/Cas9 gene editing Corrects retinal dystrophy in the S334ter-3 rat model of autosomal dominant retinitis pigmentosa. Mol. Ther. 24, 556–563.

Bannister, R.A., Beam, K.G., 2013. Ca(V)1.1: the atypical prototypical voltage-gated Ca(2)(+) channel. Biochim. Biophys. Acta 1828, 1587–1597.

Bayley, P.R., Morgans, C.W., 2007. Rod bipolar cells and horizontal cells form displaced synaptic contacts with rods in the outer nuclear layer of the nob2 retina. J. Comp. Neurol. 500, 286–298.

Bean, B.P., Sturek, M., Puga, A., Hermsmeyer, K., 1986. Calcium channels in muscle cells isolated from rat mesenteric arteries: modulation by dihydropyridine drugs. Circ. Res. 59, 229–235.

Bech-Hansen, N.T., Boycott, K.M., Gratton, K.J., Ross, D.A., Field, L.L., Pearce, W.G., 1998a. Localization of a gene for incomplete X-linked congenital stationary night blindness to the interval between DXS6849 and DXS8023 in Xp11.23. Hum. Genet. 103, 124–130.

Bech-Hansen, N.T., Naylor, M.J., Maybaum, T.A., Pearce, W.G., Koop, B., Fishman, G.A., Mets, M., Musarella, M.A., Boycott, K.M., 1998b. Loss-of-function mutations in a calcium-channel alpha1-subunit gene in Xp11.23 cause incomplete X-linked congenital stationary night blindness. Nat. Genet. 19, 264–267.

Bennett, J., 2003. Immune response following intraocular delivery of recombinant viral vectors. Gene Ther. 10, 977–982.

Berjukow, S., Hering, S., 2001. Voltage-dependent acceleration of Ca(v)1.2 channel current decay by (+)- and (-)-isradipine. Br. J. Pharmacol. 133, 959–966.

Berntson, A., Taylor, W.R., Morgans, C.W., 2003. Molecular identity, synaptic localization, and physiology of calcium channels in retinal bipolar cells. J. Neurosci. Res. 71, 146–151.

Bijveld, M.M., Florijn, R.J., Bergen, A.A., van den Born, L.I., Kamermans, M., Prick, L., Riemslag, F.C., van Schooneveld, M.J., Kappers, A.M., van Genderen, M.M., 2013. Genotype and phenotype of 101 Dutch patients with congenital stationary night blindness. Ophthalmology 120, 2072–2081.

Bock, G., Gebhart, M., Scharinger, A., Jangsangthong, W., Busquet, P., Poggiani, C., Sartori, S., Mangoni, M.E., Sinnegger-Brauns, M.J., Herzig, S., Striessnig, J., Koschak, A., 2011. Functional properties of a newly identified C-terminal splice variant of Cav1.3 L-type Ca2+ channels. J. Biol. Chem. 286, 42736–42748.

Busquet, P., Nguyen, N.K., Schmid, E., Tanimoto, N., Seeliger, M.W., Ben-Yosef, T., Mizuno, F., Akopian, A., Striessnig, J., Singewald, N., 2010. CaV1.3 L-type Ca2+ channels modulate depression-like behaviour in mice independent of deaf phenotype. Int. J. Neuropsychopharmacol. 13, 499–513.

Cabral, M.D., Paulet, P.E., Robert, V., Gomes, B., Renoud, M.L., Savignac, M., Leclerc, C., Moreau, M., Lair, D., Langelot, M., Magnan, A., Yssel, H., Mariame, B., Guery, J.C., Pelletier, L., 2010. Knocking down Cav1 calcium channels implicated in Th2 cell activation prevents experimental asthma. Am. J. Respir. Crit. Care Med. 181, 1310–1317.

Catterall, W.A., 2011. Voltage-gated calcium channels. Cold Spring Harb. Perspect. Biol. 3, a003947.

Catterall, W.A., Perez-Reyes, E., Snutch, T.P., Striessnig, J., 2005. International Union of Pharmacology. XLVIII. Nomenclature and structure-function relationships of voltage-gated calcium channels. Pharmacol. Rev. 57, 411–425.

Chan, C.S., Guzman, J.N., Ilijic, E., Mercer, J.N., Rick, C., Tkatch, T., Meredith, G.E., Surmeier, D.J., 2007. 'Rejuvenation' protects neurons in mouse models of

Parkinson's disease. Nature 447, 1081–1086.
Chang, B., Heckenlively, J.R., Bayley, P.R., Brecha, N.C., Davisson, M.T., Hawes, N.L., Hirano, A.A., Hurd, R.E., Ikeda, A., Johnson, B.A., McCall, M.A., Morgans, C.W., Nusinowitz, S., Peachey, N.S., Rice, D.S., Vessey, K.A., Gregg, R.G., 2006. The nob2 mouse, a null mutation in Cacna1f: anatomical and functional abnormalities in the outer retina and their consequences on ganglion cell visual responses. Vis. Neurosci. 23, 11–24.
Cideciyan, A.V., Aleman, T.S., Boye, S.L., Schwartz, S.B., Kaushal, S., Roman, A.J., Pang, J.J., Sumaroka, A., Windsor, E.A., Wilson, J.M., Flotte, T.R., Fishman, G.A., Heon, E., Stone, E.M., Byrne, B.J., Jacobson, S.G., Hauswirth, W.W., 2008. Human gene therapy for RPE65 isomerase deficiency activates the retinoid cycle of vision but with slow rod kinetics. Proc. Natl. Acad. Sci. U. S. A. 105, 15112–15117.
Da Costa, R., Roger, C., Segelken, J., Barben, M., Grimm, C., Neidhardt, J., 2016. A novel method combining vitreous aspiration and intravitreal AAV2/8 injection results in retina-wide transduction in adult mice. Invest Ophthalmol. Vis. Sci. 57, 5326–5334.
Dalkara, D., Byrne, L.C., Klimczak, R.R., Visel, M., Yin, L., Merigan, W.H., Flannery, J.G., Schaffer, D.V., 2013. In vivo-directed evolution of a new adeno-associated virus for therapeutic outer retinal gene delivery from the vitreous. Sci. Transl. Med. 5, 189ra176.
Davenport, B., Li, Y., Heizer, J.W., Schmitz, C., Perraud, A.L., 2015. Signature channels of excitability no more: L-type channels in immune cells. Front. Immunol. 6, 375.
Dragicevic, E., Poetschke, C., Duda, J., Schlaudraff, F., Lammel, S., Schiemann, J., Fauler, M., Hetzel, A., Watanabe, M., Lujan, R., Malenka, R.C., Striessnig, J., Liss, B., 2014. Cav1.3 channels control D2-autoreceptor responses via NCS-1 in substantia nigra dopamine neurons. Brain 137, 2287–2302.
Eden, E., Geva-Zatorsky, N., Issaeva, I., Cohen, A., Dekel, E., Danon, T., Cohen, L., Mayo, A., Alon, U., 2011. Proteome half-life dynamics in living human cells. Science 331, 764–768.
Fernandez, J.A., McGahon, M.K., McGeown, J.G., Curtis, T.M., 2015. CaV3.1 T-Type Ca2+ channels contribute to myogenic signaling in rat retinal arterioles. Invest Ophthalmol. Vis. Sci. 56, 5125–5132.
Firth, S.I., Morgan, I.G., Boelen, M.K., Morgans, C.W., 2001. Localization of voltage-sensitive L-type calcium channels in the chicken retina. Clin. Exp. Ophthalmol. 29, 183–187.
Fu, Y., Sander, J.D., Reyon, D., Cascio, V.M., Joung, J.K., 2014. Improving CRISPR-Cas nuclease specificity using truncated guide RNAs. Nat. Biotechnol. 32, 279–284.
Grabner, C.P., Gandini, M.A., Rehak, R., Le, Y., Zamponi, G.W., Schmitz, F., 2015. RIM1/2-Mediated facilitation of Cav1.4 channel opening is required for Ca2+-Stimulated release in mouse rod photoreceptors. J. Neurosci. 35, 13133–13147.
Gruntman, A.M., Bish, L.T., Mueller, C., Sweeney, H.L., Flotte, T.R., Gao, G., 2013. Gene transfer in skeletal and cardiac muscle using recombinant adeno-associated virus. Curr. Protoc. Microbiol. http://dx.doi.org/10.1002/9780471729259.mc14d03s28. Chapter 14, Unit 14D.3.
Haeseleer, F., Imanishi, Y., Maeda, T., Possin, D.E., Maeda, A., Lee, A., Rieke, F., Palczewski, K., 2004. Essential role of Ca2+-binding protein 4, a Cav1.4 channel regulator, in photoreceptor synaptic function. Nat. Neurosci. 7, 1079–1087.
Haeseleer, F., Williams, B., Lee, A., 2016. Characterization of C-terminal splice variants of Cav1.4 Ca2+ channels in human retina. J. Biol. Chem. 291, 15663–15673.
Hamilton, S.L., Yatani, A., Brush, K., Schwartz, A., Brown, A.M., 1987. A comparison between the binding and electrophysiological effects of dihydropyridines on cardiac membranes. Mol. Pharmacol. 31, 221–231.
Harraz, O.F., Brett, S.E., Zechariah, A., Romero, M., Puglisi, J.L., Wilson, S.M., Welsh, D.G., 2015a. Genetic ablation of CaV3.2 channels enhances the arterial myogenic response by modulating the RyR-BKCa axis. Arterioscler. Thromb. Vasc. Biol. 35, 1843–1851.
Harraz, O.F., Visser, F., Brett, S.E., Goldman, D., Zechariah, A., Hashad, A.M., Menon, B.K., Watson, T., Starreveld, Y., Welsh, D.G., 2015b. CaV1.2/CaV3.x channels mediate divergent vasomotor responses in human cerebral arteries. J. Gen. Physiol. 145, 405–418.
Hasan, N., Ray, T.A., Gregg, R.G., 2016. CACNA1S expression in mouse retina: novel isoforms and antibody cross-reactivity with GPR179. Vis. Neurosci. 33, E009.
Hemara-Wahanui, A., Berjukow, S., Hope, C.I., Dearden, P.K., Wu, S.B., Wilson-Wheeler, J., Sharp, D.M., Lundon-Treweek, P., Clover, G.M., Hoda, J.C., Striessnig, J., Marksteiner, R., Hering, S., Maw, M.A., 2005. A CACNA1F mutation identified in an X-linked retinal disorder shifts the voltage dependence of Cav1.4 channel activation. Proc. Natl. Acad. Sci. U. S. A. 102, 7553–7558.
Hofmann, F., Flockerzi, V., Kahl, S., Wegener, J.W., 2014. L-type CaV1.2 calcium channels: from in vitro findings to in vivo function. Physiol. Rev. 94, 303–326.
Hope, C.I., Sharp, D.M., Hemara-Wahanui, A., Sissingh, J.I., Lundon, P., Mitchell, E.A., Maw, M.A., Clover, G.M., 2005. Clinical manifestations of a unique X-linked retinal disorder in a large New Zealand family with a novel mutation in CACNA1F, the gene responsible for CSNB2. Clin. Exp. Ophthalmol. 33, 129–136.
Hu, Z., Wang, J.W., Yu, D., Soon, J.L., de Kleijn, D.P., Foo, R., Liao, P., Colecraft, H.M., Soong, T.W., 2016. Aberrant splicing promotes proteasomal degradation of L-type CaV1.2 calcium channels by Competitive binding for CaVbeta subunits in cardiac hypertrophy. Sci. Rep. 6, 35247.
Huang, H., Ng, C.Y., Yu, D., Zhai, J., Lam, Y., Soong, T.W., 2014. Modest CaV1.342-selective inhibition by compound 8 is beta-subunit dependent. Nat. Commun. 5, 4481.
Hung, S.S., Chrysostomou, V., Li, F., Lim, J.K., Wang, J.H., Powell, J.E., Tu, L., Daniszewski, M., Lo, C., Wong, R.C., Crowston, J.G., Pebay, A., King, A.E., Bui, B.V., Liu, G.S., Hewitt, A.W., 2016. AAV-mediated CRISPR/Cas gene editing of retinal cells in vivo. Invest Ophthalmol. Vis. Sci. 57, 3470–3476.
Ivanova, E., Hwang, G.S., Pan, Z.H., 2010. Characterization of transgenic mouse lines expressing Cre recombinase in the retina. Neuroscience 165, 233–243.
Jha, A., Singh, A.K., Weissgerber, P., Freichel, M., Flockerzi, V., Flavell, R.A., Jha, M.K., 2015. Essential roles for Cavbeta2 and Cav1 channels in thymocyte development and T cell homeostasis. Sci. Signal 8, ra103.
Jia, S., Muto, A., Orisme, W., Henson, H.E., Parupalli, C., Ju, B., Baier, H., Taylor, M.R., 2014. Zebrafish Cacna1fa is required for cone photoreceptor function and synaptic ribbon formation. Hum. Mol. Genet. 23, 2981–2994.
Jurkat-Rott, K., Lerche, H., Lehmann-Horn, F., 2002. Skeletal muscle channelopathies. J. Neurol. 249, 1493–1502.
Knoflach, D., Kerov, V., Sartori, S.B., Obermair, G.J., Schmuckermair, C., Liu, X., Sothilingam, V., Garrido, M.G., Baker, S.A., Glosmann, M., Schicker, K., Seeliger, M., Lee, A., Koschak, A., 2013. Cav1.4 IT mouse as model for vision impairment in human congenital stationary night blindness type 2. Channels (Austin) 7, 503–513.
Knoflach, D., Schicker, K., Glosmann, M., Koschak, A., 2015. Gain-of-function nature of Cav1.4 L-type calcium channels alters firing properties of mouse retinal ganglion cells. Channels (Austin) 9, 298–306.
Koch, S., Sothilingam, V., Garcia Garrido, M., Tanimoto, N., Becirovic, E., Koch, F., Seide, C., Beck, S.C., Seeliger, M.W., Biel, M., Muhlfriedel, R., Michalakis, S., 2012. Gene therapy restores vision and delays degeneration in the CNGB1(-/-) mouse model of retinitis pigmentosa. Hum. Mol. Genet. 21, 4486–4496.
Koschak, A., Reimer, D., Huber, I., Grabner, M., Glossmann, H., Engel, J., Striessnig, J., 2001. α1D (Ca_v1.3) subunits can form L-type Ca^{2+} channels activating at negative voltages. J. Biol. Chem. 276, 22100–22106.
Koschak, A., Reimer, D., Walter, D., Hoda, J.C., Heinzle, T., Grabner, M., Striessnig, J., 2003. Ca_v1.4α1 subunits can form slowly inactivating dihydropyridine-sensitive L-type Ca^{2+} channels lacking Ca^{2+}-dependent inactivation. J. Neurosci. 23, 6041–6049.
Kotturi, M.F., Jefferies, W.A., 2005. Molecular characterization of L-type calcium channel splice variants expressed in human T lymphocytes. Mol. Immunol. 42, 1461–1474.
Kuo, I.Y., Howitt, L., Sandow, S.L., McFarlane, A., Hansen, P.B., Hill, C.E., 2014. Role of T-type channels in vasomotor function: team player or chameleon? Pflugers Arch. 466, 767–779.
Latella, M.C., Di Salvo, M.T., Cocchiarella, F., Benati, D., Grisendi, G., Comitato, A., Marigo, V., Recchia, A., 2016. In vivo editing of the human mutant rhodopsin gene by electroporation of plasmid-based CRISPR/Cas9 in the mouse retina. Mol. Ther. Nucleic Acids 5, e389.
Li, Q., Miller, R., Han, P.Y., Pang, J., Dinculescu, A., Chiodo, V., Hauswirth, W.W., 2008. Intraocular route of AAV2 vector administration defines humoral immune response and therapeutic potential. Mol. Vis. 14, 1760–1769.
Liao, P., Li, G., Yu de, J., Yong, T.F., Wang, J.J., Wang, J., Soong, T.W., 2009. Molecular alteration of Ca(v)1.2 calcium channel in chronic myocardial infarction. Pflugers Arch. 458, 701–711.
Liu, X., Kerov, V., Haeseleer, F., Majumder, A., Artemyev, N., Baker, S.A., Lee, A., 2013. Dysregulation of Ca(v)1.4 channels disrupts the maturation of photoreceptor synaptic ribbons in congenital stationary night blindness type 2. Channels (Austin) 7, 514–523.
Lizio, M., Harshbarger, J., Shimoji, H., Severin, J., Kasukawa, T., Sahin, S., Abugessaisa, I., Fukuda, S., Hori, F., Ishikawa-Kato, S., Mungall, C.J., Arner, E., Baillie, J.K., Bertin, N., Bono, H., de Hoon, M., Diehl, A.D., Dimont, E., Freeman, T.C., Fujieda, K., Hide, W., Kaliyaperumal, R., Katayama, T., Lassmann, T., Meehan, T.F., Nishikata, K., Ono, H., Rehli, M., Sandelin, A., Schultes, E.A., t Hoen, P.A., Tatum, Z., Thompson, M., Toyoda, T., Wright, D.W., Daub, C.O., Itoh, M., Carninci, P., Hayashizaki, Y., Forrest, A.R., Kawaji, H., consortium, F., 2015. Gateways to the FANTOM5 promoter level mammalian expression atlas. Genome Biol. 16, 22.
Lu, Q.L., Bou-Gharios, G., Partridge, T.A., 2003. Non-viral gene delivery in skeletal muscle: a protein factory. Gene Ther. 10, 131–142.
Maguire, A.M., Simonelli, F., Pierce, E.A., Pugh Jr., E.N., Mingozzi, F., Bennicelli, J., Banfi, S., Marshall, K.A., Testa, F., Surace, E.M., Rossi, S., Lyubarsky, A., Arruda, V.R., Konkle, B., Stone, E., Sun, J., Jacobs, J., Dell'Osso, L., Hertle, R., Ma, J.X., Redmond, T.M., Zhu, X., Hauck, B., Zelenaia, O., Shindler, K.S., Maguire, M.G., Wright, J.F., Volpe, N.J., McDonnell, J.W., Auricchio, A., High, K.A., Bennett, J., 2008. Safety and efficacy of gene transfer for Leber's congenital amaurosis. N. Engl. J. Med. 358, 2240–2248.
Mangoni, M.E., Couette, B., Bourinet, E., Platzer, J., Reimer, D., Striessnig, J., Nargeot, J., 2003. Functional role of L-type Ca_v1.3 Ca^{2+} channels in cardiac pacemaker activity. Proc. Natl. Acad. Sci. U. S. A. 100, 5543–5548.
Mansergh, F., Orton, N.C., Vessey, J.P., Lalonde, M.R., Stell, W.K., Tremblay, F., Barnes, S., Rancourt, D.E., Bech-Hansen, N.T., 2005. Mutation of the calcium channel gene Cacna1f disrupts calcium signaling, synaptic transmission and cellular organization in mouse retina. Hum. Mol. Genet. 14, 3035–3046.
Marcantoni, A., Vandael, D. H., Mahapatra, S., Carabelli, V., Sinnegger-Brauns, M. J., Striessnig, J., Carbone, E., Loss of Cav1.3 channels reveals the critical role of L-type and BK channel coupling in pacemaking mouse adrenal chromaffin cells. J. Neurosci. 30, 491–504.
Matza, D., Badou, A., Klemic, K.G., Stein, J., Govindarajulu, U., Nadler, M.J., Kinet, J.P., Peled, A., Shapira, O.M., Kaczmarek, L.K., Flavell, R.A., 2016. T cell receptor mediated calcium entry requires alternatively spliced Cav1.1 channels. PLoS One 11, e0147379.
McRory, J.E., Hamid, J., Doering, C.J., Garcia, E., Parker, R., Hamming, K., Chen, L., Hildebrand, M., Beedle, A.M., Feldcamp, L., Zamponi, G.W., Snutch, T.P., 2004. The CACNA1F gene encodes an L-type calcium channel with unique biophysical

properties and tissue distribution. J. Neurosci. 24, 1707–1718.
Michalakis, S., Muhlfriedel, R., Tanimoto, N., Krishnamoorthy, V., Koch, S., Fischer, M.D., Becirovic, E., Bai, L., Huber, G., Beck, S.C., Fahl, E., Buning, H., Paquet-Durand, F., Zong, X., Gollisch, T., Biel, M., Seeliger, M.W., 2010. Restoration of cone vision in the CNGA3-/- mouse model of congenital complete lack of cone photoreceptor function. Mol. Ther. 18, 2057–2063.
Michalakis, S., Shaltiel, L., Sothilingam, V., Koch, S., Schludi, V., Krause, S., Zeitz, C., Audo, I., Lancelot, M.E., Hamel, C., Meunier, I., Preising, M.N., Friedburg, C., Lorenz, B., Zabouri, N., Haverkamp, S., Garcia Garrido, M., Tanimoto, N., Seeliger, M.W., Biel, M., Wahl-Schott, C.A., 2014. Mosaic synaptopathy and functional defects in Cav1.4 heterozygous mice and human carriers of CSNB2. Hum. Mol. Genet. 23, 1538–1550.
Miyake, Y., 2002. Establishment of the concept of new clinical entities–complete and incomplete form of congenital stationary night blindness. Nippon. Ganka Gakkai Zasshi 106, 737–755 discussion 756.
Miyake, Y., Yagasaki, K., Horiguchi, M., Kawase, Y., Kanda, T., 1986. Congenital stationary night blindness with negative electroretinogram. A new classification. Arch. Ophthalmol. 104, 1013–1020.
Moosmang, S., Schulla, V., Welling, A., Feil, R., Feil, S., Wegener, J.W., Hofmann, F., Klugbauer, N., 2003. Dominant role of smooth muscle L-type calcium channel Cav1.2 for blood pressure regulation. EMBO J. 22, 6027–6034.
Morgans, C.W., Bayley, P.R., Oesch, N.W., Ren, G., Akileswaran, L., Taylor, W.R., 2005. Photoreceptor calcium channels: insight from night blindness. Vis. Neurosci. 22, 561–568.
Morgans, C.W., Gaughwin, P., Maleszka, R., 2001. Expression of the alpha1F calcium channel subunit by photoreceptors in the rat retina. Mol. Vis. 7, 202–209.
Muller, C., Mas Gomez, N., Ruth, P., Strauss, O., 2014. CaV1.3 L-type channels, maxiK Ca(2+)-dependent K(+) channels and bestrophin-1 regulate rhythmic photoreceptor outer segment phagocytosis by retinal pigment epithelial cells. Cell Signal 26, 968–978.
Olson, P.A., Tkatch, T., Hernandez-Lopez, S., Ulrich, S., Ilijic, E., Mugnaini, E., Zhang, H., Bezprozvanny, I., Surmeier, D.J., 2005. G-protein-coupled receptor modulation of striatal $Ca_v1.3$ L-type Ca^{2+} channels is dependent on a Shank-binding domain. J. Neurosci. 25, 1050–1062.
Omilusik, K., Priatel, J.J., Chen, X., Wang, Y.T., Xu, H., Choi, K.B., Gopaul, R., McIntyre-Smith, A., Teh, H.S., Tan, R., Bech-Hansen, N.T., Waterfield, D., Fedida, D., Hunt, S.V., Jefferies, W.A., 2011. The Ca(v)1.4 calcium channel is a critical regulator of T cell receptor signaling and naive T cell homeostasis. Immunity 35, 349–360.
Ortner, N.J., Bock, G., Dougalis, A., Kharitonova, M., Duda, J., Hess, S., Tuluc, P., Pomberger, T., Stefanova, N., Pitterl, F., Ciossek, T., Oberacher, H., Draheim, H.J., Kloppenburg, P., Liss, B., Striessnig, J., 2017 Jun 7. Lower affinity of isradipine for L-type Ca2+ channels during substantia nigra dopamine neuron-like activity: implications for neuroprotection in Parkinson's disease. J. Neurosci. http://dx.doi.org/10.1523/JNEUROSCI.2946-16.2017 pii: 2946-16. [Epub ahead of print].
Qiao, C., Koo, T., Li, J., Xiao, X., Dickson, J.G., 2011. Gene therapy in skeletal muscle mediated by adeno-associated virus vectors. Methods Mol. Biol. 807, 119–140.
Rabl, K., Thoreson, W.B., 2002. Calcium-dependent inactivation and depletion of synaptic cleft calcium ions combine to regulate rod calcium currents under physiological conditions. Eur. J. Neurosci. 16, 2070–2077.
Raven, M.A., Orton, N.C., Nassar, H., Williams, G.A., Stell, W.K., Jacobs, G.H., Bech-Hansen, N.T., Reese, B.E., 2008. Early afferent signaling in the outer plexiform layer regulates development of horizontal cell morphology. J. Comp. Neurol. 506, 745–758.
Regus-Leidig, H., Atorf, J., Feigenspan, A., Kremers, J., Maw, M.A., Brandstatter, J.H., 2014. Photoreceptor degeneration in two mouse models for congenital stationary night blindness type 2. PLoS One 9, e86769.
Robert, V., Triffaux, E., Paulet, P.E., Guery, J.C., Pelletier, L., Savignac, M., 2014. Protein kinase C-dependent activation of CaV1.2 channels selectively controls human TH2-lymphocyte functions. J. Allergy Clin. Immunol. 133, 1175–1183.
Ruan, G.X., Barry, E., Yu, D., Lukason, M., Cheng, S.H., Scaria, A., 2017. CRISPR/Cas9-Mediated genome editing as a therapeutic approach for Leber congenital amaurosis 10. Mol. Ther. 25, 331–341.
Saada, Y.B., Dib, C., Lipinski, M., Vassetzky, Y.S., 2016. Genome- and cell-based strategies in therapy of muscular dystrophies. Biochem. (Mosc) 81, 678–690.
Santoro, M., Piacentini, R., Masciullo, M., Bianchi, M.L., Modoni, A., Podda, M.V., Ricci, E., Silvestri, G., Grassi, C., 2014. Alternative splicing alterations of Ca2+ handling genes are associated with Ca2+ signal dysregulation in myotonic dystrophy type 1 (DM1) and type 2 (DM2) myotubes. Neuropathol. Appl. Neurobiol. 40, 464–476.
Schlick, B., Flucher, B.E., Obermair, G.J., 2010. Voltage-activated calcium channel expression profiles in mouse brain and cultured hippocampal neurons. Neuroscience 167, 786–798.
Scholl, H.P., Strauss, R.W., Singh, M.S., Dalkara, D., Roska, B., Picaud, S., Sahel, J.A., 2016. Emerging therapies for inherited retinal degeneration. Sci. Transl. Med. 8, 368rv366.
Sengillo, J.D., Justus, S., Cabral, T., Tsang, S.H., 2017. Correction of monogenic and common retinal disorders with gene therapy. Genes (Basel) 8.
Siegert, S., Cabuy, E., Scherf, B.G., Kohler, H., Panda, S., Le, Y.Z., Fehling, H.J., Gaidatzis, D., Stadler, M.B., Roska, B., 2012. Transcriptional code and disease map for adult retinal cell types. Nat. Neurosci. 15 (487–495), S481–S482.
Singh, A., Gebhart, M., Fritsch, R., Sinnegger-Brauns, M.J., Poggiani, C., Hoda, J.C., Engel, J., Romanin, C., Striessnig, J., Koschak, A., 2008 Jul 25. Modulation of voltage- and Ca2+-dependent gating of CaV1.3 L-type calcium channels by alternative splicing of a C-terminal regulatory domain. J. Biol. Chem. 283 (30), 20733–20744.
Singh, A., Hamedinger, D., Hoda, J.C., Gebhart, M., Koschak, A., Romanin, C., Striessnig, J., 2006. C-terminal modulator controls Ca^{2+}-dependent gating of $Ca_v1.4$ L-type Ca^{2+} channels. Nat. Neurosci. 9, 1108–1116.
Sinnegger-Brauns, M.J., Huber, I.G., Koschak, A., Wild, C., Obermair, G.J., Einzinger, U., Hoda, J.C., Sartori, S.B., Striessnig, J., 2009. Expression and 1,4-dihydropyridine-binding properties of brain L-type calcium channel isoforms. Mol. Pharmacol. 75, 407–414.
Sommese, L., Zullo, A., Schiano, C., Mancini, F.P., Napoli, C., 2017 Apr. Possible muscle repair in the human cardiovascular system. Stem Cell Rev. 13 (2), 170–191.
Southan, C., Sharman, J.L., Benson, H.E., Faccenda, E., Pawson, A.J., Alexander, S.P., Buneman, O.P., Davenport, A.P., McGrath, J.C., Peters, J.A., Spedding, M., Catterall, W.A., Fabbro, D., Davies, J.A., Nc, I., 2016. The IUPHAR/BPS Guide to PHARMACOLOGY in 2016: towards curated quantitative interactions between 1300 protein targets and 6000 ligands. Nucleic Acids Res. 44, D1054–D1068.
Specht, D., Wu, S.B., Turner, P., Dearden, P., Koentgen, F., Wolfrum, U., Maw, M., Brandstatter, J.H., tom Dieck, S., 2009. Effects of presynaptic mutations on a postsynaptic Cacna1s calcium channel colocalized with mGluR6 at mouse photoreceptor ribbon synapses. Invest Ophthalmol. Vis. Sci. 50, 505–515.
Striessnig, J., 2007. C-terminal tailoring of L-type calcium channel function. J. Physiol. 585, 643–644.
Striessnig, J., Koschak, A., 2008. Exploring the function and pharmacotherapeutic potential of voltage-gated Ca2+ channels with gene knockout models. Channels (Austin) 2, 233–251.
Striessnig, J., Ortner, N.J., Pinggera, A., 2015. Pharmacology of L-type calcium channels: novel drugs for old targets? Curr. Mol. Pharmacol. 8, 110–122.
Subramanyam, P., Chang, D.D., Fang, K., Xie, W., Marks, A.R., Colecraft, H.M., 2013. Manipulating L-type calcium channels in cardiomyocytes using split-intein protein transsplicing. Proc. Natl. Acad. Sci. U. S. A. 110, 15461–15466.
Tan, G.M., Yu, D., Wang, J., Soong, T.W., 2012. Alternative splicing at C terminus of Ca(V)1.4 calcium channel modulates calcium-dependent inactivation, activation potential, and current density. J. Biol. Chem. 287, 832–847.
Tang, Z.Z., Yarotskyy, V., Wei, L., Sobczak, K., Nakamori, M., Eichinger, K., Moxley, R.T., Dirksen, R.T., Thornton, C.A., 2012. Muscle weakness in myotonic dystrophy associated with misregulated splicing and altered gating of Ca(V)1.1 calcium channel. Hum. Mol. Genet. 21, 1312–1324.
Tuluc, P., Molenda, N., Schlick, B., Obermair, G.J., Flucher, B.E., Jurkat-Rott, K., 2009. A CaV1.1 Ca2+ channel splice variant with high conductance and voltage-sensitivity alters EC coupling in developing skeletal muscle. Biophys. J. 96, 35–44.
Tummala, S.R., Neinstein, A., Fina, M.E., Dhingra, A., Vardi, N., 2014. Localization of Cacna1s to ON bipolar dendritic tips requires mGluR6-related cascade elements. Invest Ophthalmol. Vis. Sci. 55, 1483–1492.
Uhlen, M., Fagerberg, L., Hallstrom, B.M., Lindskog, C., Oksvold, P., Mardinoglu, A., Sivertsson, A., Kampf, C., Sjostedt, E., Asplund, A., Olsson, I., Edlund, K., Lundberg, E., Navani, S., Szigyarto, C.A., Odeberg, J., Djureinovic, D., Takanen, J.O., Hober, S., Alm, T., Edqvist, P.H., Berling, H., Tegel, H., Mulder, J., Rockberg, J., Nilsson, P., Schwenk, J.M., Hamsten, M., von Feilitzen, K., Forsberg, M., Persson, L., Johansson, F., Zwahlen, M., von Heijne, G., Nielsen, J., Ponten, F., 2015. Proteomics. Tissue-based map of the human proteome. Science 347, 1260419.
Uhlen, M., Hallstrom, B.M., Lindskog, C., Mardinoglu, A., Ponten, F., Nielsen, J., 2016. Transcriptomics resources of human tissues and organs. Mol. Syst. Biol. 12, 862.
von Gersdorff, H., Matthews, G., 1996. Calcium-dependent inactivation of calcium current in synaptic terminals of retinal bipolar neurons. J. Neurosci. 16, 115–122.
Wahl-Schott, C., Baumann, L., Cuny, H., Eckert, C., Griessmeier, K., Biel, M., 2006. Switching off calcium-dependent inactivation in L-type calcium channels by an autoinhibitory domain. Proc. Natl. Acad. Sci. U. S. A. 103, 15657–15662.
Wang, D., Papp, A.C., Binkley, P.F., Johnson, J.A., Sadee, W., 2006. Highly variable mRNA expression and splicing of L-type voltage-dependent calcium channel alpha subunit 1C in human heart tissues. Pharmacogenet Genomics 16, 735–745.
Wang, D., Zhong, L., Nahid, M.A., Gao, G., 2014. The potential of adeno-associated viral vectors for gene delivery to muscle tissue. Expert Opin. Drug Deliv. 11, 345–364.
Welling, A., Ludwig, A., Zimmer, S., Klugbauer, N., Flockerzi, V., Hofmann, F., 1997. Alternatively spliced IS6 segments of the alpha 1C gene determine the tissue-specific dihydropyridine sensitivity of cardiac and vascular smooth muscle L-type Ca2+ channels. Circ. Res. 81, 526–532.
Wilhelm, M., Schlegl, J., Hahne, H., Gholami, A.M., Lieberenz, M., Savitski, M.M., Ziegler, E., Butzmann, L., Gessulat, S., Marx, H., Mathieson, T., Lemeer, S., Schnatbaum, K., Reimer, U., Wenschuh, H., Mollenhauer, M., Slotta-Huspenina, J., Boese, J.H., Bantscheff, M., Gerstmair, A., Faerber, F., Kuster, B., 2014. Mass-spectrometry-based draft of the human proteome. Nature 509, 582–587.
Wimmers, S., Coeppicus, L., Rosenthal, R., Strauss, O., 2008. Expression profile of voltage-dependent Ca2+ channel subunits in the human retinal pigment epithelium. Graefes Arch. Clin. Exp. Ophthalmol. 246, 685–692.
Xu, W., Lipscombe, D., 2001. Neuronal $Ca_v1.3\alpha1$ L-type channels activate at relatively hyperpolarized membrane potentials and are incompletely inhibited by dihydropyridines. J. Neurosci. 21, 5944–5951.
Yanik, M., Muller, B., Song, F., Gall, J., Wagner, F., Wende, W., Lorenz, B., Stieger, K., 2017. In vivo genome editing as a potential treatment strategy for inherited retinal dystrophies. Prog. Retin Eye Res. 56, 1–18.

Yu, H., Seo, J.B., Jung, S.R., Koh, D.S., Hille, B., 2015a. Noradrenaline upregulates T-type calcium channels in rat pinealocytes. J. Physiol. 593, 887–904.
Yu, N.Y., Hallstrom, B.M., Fagerberg, L., Ponten, F., Kawaji, H., Carninci, P., Forrest, A.R., Fantom, C., Hayashizaki, Y., Uhlen, M., Daub, C.O., 2015b. Complementing tissue characterization by integrating transcriptome profiling from the Human Protein Atlas and from the FANTOM5 consortium. Nucleic Acids Res. 43, 6787–6798.
Zabouri, N., Haverkamp, S., 2013. Calcium channel-dependent molecular maturation of photoreceptor synapses. PLoS One 8, e63853.
Zamponi, G.W., Striessnig, J., Koschak, A., Dolphin, A.C., 2015. The physiology, pathology, and pharmacology of voltage-gated calcium channels and their future therapeutic potential. Pharmacol. Rev. 67, 821–870.
Zeitz, C., Robson, A.G., Audo, I., 2015. Congenital stationary night blindness: an analysis and update of genotype-phenotype correlations and pathogenic mechanisms. Prog. Retin Eye Res. 45, 58–110.
Zhang, J., Berra-Romani, R., Sinnegger-Brauns, M.J., Striessnig, J., Blaustein, M.P., Matteson, D.R., 2007 Jan. Role of Cav1.2 L-type Ca2+ channels in vascular tone: effects of nifedipine and Mg2+. Am. J. Physiol. Heart Circ. Physiol. 292 (1), H415–H425.